

Strong Magnetophotovoltaic Effect in Folded Graphene

Friedemann Queisser and Ralf Schützhold*

Fakultät für Physik, Universität Duisburg-Essen, Lotharstrasse 1, 47057 Duisburg, Germany

(Received 28 January 2013; published 22 July 2013)

We study electronic transport in graphene under the influence of a transversal magnetic field $\mathbf{B}(\mathbf{r}) = B(x)\mathbf{e}_z$ with the asymptotics $B(x \rightarrow \pm\infty) = \pm B_0$, which could be realized via a folded graphene sheet in a constant magnetic field, for example. By solving the effective Dirac equation, we find robust modes with a finite energy gap which propagate along the fold—where particles and holes move in opposite directions. Exciting these particle-hole pairs with incident (optical or infrared) photons would then generate a nearly perfect charge separation and thus a strong magnetophotovoltaic or magnetothermoelectric effect—even at room temperature.

DOI: 10.1103/PhysRevLett.111.046601

PACS numbers: 72.80.Vp, 78.67.Wj, 85.80.Fi

Introduction.—Photoelectric or thermoelectric effects facilitate the direct conversion of light or heat into electric energy and thus are of general interest. Obviously, the \mathcal{C} (charge), \mathcal{P} (parity), and \mathcal{T} (time reversal) symmetries must be broken for such an effect to occur. One way to achieve this is with a magnetic field [1] in a suitable geometry: trajectories of opposite charge carriers are bent to antipodal directions. However, the mean free path in usual materials is too short to generate an efficient charge separation in that way—at least at room temperature. For example, the classical cyclotron radius $r = m_e v / (q_e B)$ of a free electron at room temperature in a magnetic field B of 1 T [$r = \mathcal{O}(\mu\text{m})$] is much larger than the typical mean free path (in the nanometer range). Thus, these effects are strongly suppressed by multiple scattering events and dissipation, etc.

This motivates the study of graphene [2–6], since this system offers a comparably long mean free path and a large electron mobility, a linear (pseudorelativistic) dispersion relation at low energies (i.e., near the Dirac points), and a very large Fermi velocity $v_F \approx 10^6$ m/s [3] (see also Refs. [7,8]). In this case, the pseudorelativistic cyclotron radius at room temperature in a magnetic field of 1 T is much smaller (some tens of nanometers). In this regime, quantum effects should be taken into account—even at room temperature [4].

In the following, we consider folded graphene in a transversal magnetic field (see Fig. 1). In principle, the folding of graphene has already been realized experimentally (see, e.g., Refs. [9,10]). This setup is advantageous since we avoid real edges in graphene which are typically not perfect and contain cracks or other defects which might induce scattering, coupling to vibrational degrees of freedom, or further unwanted effects. From a theoretical point of view, these edges can only be described in idealized cases, e.g., via effective boundary conditions which then depend on the concrete realization (e.g., zigzag or armchair structure [11–13]). The fold is supposed to be terminated by two metallic leads (with chemical potentials equal to the

Dirac point of graphene) which allow us to measure the generated current.

Eigenmodes.—We consider length scales (e.g., curvature radius of fold) far above the lattice spacing of graphene ≈ 0.25 nm and energies of 1 eV or below. In this limit, we may describe the low-energy behavior by an effective Dirac equation in $2 + 1$ dimensions ($\hbar = q_e = 1$)

$$i\gamma^\mu(\partial_\mu + iA_\mu)\Psi = 0, \quad (1)$$

with $x^\mu = [v_F t, x, y]$, where $v_F \approx 10^6$ m/s is the Fermi velocity [14,15]. The Dirac matrices $\gamma^\mu = [\sigma^z, i\sigma^y, -i\sigma^x]$ acting on $\Psi = [\psi_1, \psi_2]$ are related to the Pauli matrices $\sigma^{x,y,z}$. In the Landau gauge, the vector potential $A_\mu = [0, 0, A(x)]$ generates the magnetic field $B(x) = \partial_x A(x)$ with the asymptotics $B(x \rightarrow \pm\infty) = \pm B_0$.

In view of the translation symmetry in t and y [16], we can make the separation ansatz for the modes

$$\Psi(t, x, y) = \exp\{-iEt +iky\}\Psi^{E,k}(x), \quad (2)$$

arriving at the two coupled equations

$$\begin{aligned} iv_F[\partial_x + k + A(x)]\psi_2^{E,k}(x) &= E\psi_1^{E,k}(x), \\ iv_F[\partial_x - k - A(x)]\psi_1^{E,k}(x) &= E\psi_2^{E,k}(x). \end{aligned} \quad (3)$$

Hence, we can choose $\psi_1^{E,k}(x)$ to be real, for example, while $\psi_2^{E,k}(x)$ is imaginary. We observe a particle-hole symmetry since replacing $E \rightarrow -E$ and $\psi_2^{E,k} \rightarrow -\psi_2^{E,k}$ yields a new solution $\Psi^{-E,k} = \sigma^z \Psi^{E,k} = (\Psi^{E,k})^*$.

The two first-order equations (3) can be combined into one second-order equation

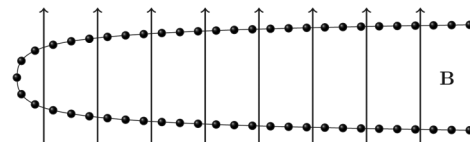


FIG. 1. Sketch of the considered setup.

$$v_F^2[k + A(x) + \partial_x][k + A(x) - \partial_x]\psi_1^{E,k} = E^2\psi_1^{E,k}, \quad (4)$$

and analogously for $\psi_2^{E,k}$ with $\partial_x \leftrightarrow -\partial_x$. This equation can be cast into the form of a one-dimensional Schrödinger equation $\mathcal{H}_k\psi_1^{E,k} = E^2\psi_1^{E,k}$ with the Hamiltonian $\mathcal{H}_k = v_F^2(-\partial_x^2 + \mathcal{V}_k)$ containing the effective potential $\mathcal{V}_k = [k + A(x)]^2 + A'(x)$. Since this Hamiltonian is self-adjoint $\mathcal{H}_k = \mathcal{H}_k^\dagger$ and the potential \mathcal{V}_k has the asymptotics $\mathcal{V}_k(x \rightarrow \pm\infty) = \infty$, we get a complete set of discrete, orthonormal, and localized (in x) eigenfunctions $\psi_1^{E,k}(x)$ for every value of k . These modes are non-degenerate for each k ; i.e., the energy bands $E(k)$ do not cross [17]. Because of the particle-hole symmetry, each of these eigenfunctions $\psi_1^{E,k}(x)$ corresponds to a pair of modes $\Psi^{\pm E,k}(x)$ of the original problem (3) with opposite energies. Furthermore, with $\mathcal{D}_k = k + A(x) - \partial_x$, we may write $\mathcal{H}_k = v_F^2\mathcal{D}_k^\dagger\mathcal{D}_k$ which shows that \mathcal{H}_k is nonnegative (and thus E is real). In addition, \mathcal{H}_k cannot have a zero eigenvalue $E = 0$ since the corresponding $\psi_1^{E=0,k}(x)$ must satisfy $\mathcal{D}_k\psi_1^{E=0,k} = 0$, which gives $\psi_1^{E=0,k}(x) \propto \exp\{kx + \int dx A(x)\}$ and analogously for $\psi_2^{E=0,k}(x)$. Due to the asymptotics $B(x \rightarrow \pm\infty) = \pm B_0$ and thus $A(x \rightarrow \pm\infty) \sim B_0|x|$, this solution is not normalizable and thus \mathcal{H}_k is strictly positive for any k . Ergo, the modes do always have a finite energy gap $E \neq 0$.

Current.—The current density of the modes reads

$$j_{E,k}^\mu = v_F \bar{\Psi}_{E,k} \gamma^\mu \Psi_{E,k} = v_F \Psi_{E,k}^\dagger \gamma^0 \gamma^\mu \Psi_{E,k}. \quad (5)$$

The zeroth component $j^0 = v_F \rho$ is simply given by the density $\rho = |\psi_1^{E,k}|^2 + |\psi_2^{E,k}|^2$. As one would expect, j^x vanishes identically since $\psi_1^{E,k}(x)$ is real and $\psi_2^{E,k}(x)$ is imaginary [cf. Eq. (3)]. Using the same argument, the current density in the y direction simplifies to

$$j^y = i v_F (\psi_2^{E,k})^* \psi_1^{E,k} - \text{H.c.} = -2i v_F \psi_1^{E,k} \psi_2^{E,k}. \quad (6)$$

From the triangle inequality ($2|ab| \leq |a^2| + |b^2|$), we may infer $|j^y| \leq v_F \rho$; i.e., the speed of the associated charge carriers is at most the Fermi velocity v_F (as expected).

The total current in the y direction can be obtained by

$$J^y = \int dx j^y = -\frac{2v_F^2}{E} \int dx \psi_1^{E,k} [k + A(x)] \psi_1^{E,k}, \quad (7)$$

where we have used $v_F \mathcal{D}_k \psi_1^{E,k} = iE \psi_2^{E,k}$ from Eq. (3). For the lowest E^2 modes (for a given k), i.e., the uppermost negative mode and the lowermost positive mode, the wave function $\psi_1^{E,k}(x)$ corresponds to the ground state of \mathcal{H}_k and hence it is nonzero for all x (node theorem [17]). Since one can repeat the same line of argument for $\psi_2^{E,k}(x)$, the integrand $j^y = -2i v_F \psi_1^{E,k} \psi_2^{E,k}$ is nonzero for all x and hence the current J^y is finite. But other modes could have $J^y = 0$ at some k value. However, for large enough $k > -A_{\min} = -\min\{A(x)\}$, the integrand in the above

equation $\psi_1^{E,k}[k + A(x)]\psi_1^{E,k}$ is positive for all x and thus the current has a finite value.

Furthermore, the current J^y is related to the slope dE/dk of the dispersion relation, i.e., the group velocity. Writing Eq. (3) as $\hat{H}_{E,k}|\Psi_{E,k}\rangle = E|\Psi_{E,k}\rangle$, we find

$$J^y = -\langle \Psi_{E,k} | \frac{d\hat{H}_{E,k}}{dk} | \Psi_{E,k} \rangle = -\frac{dE}{dk}, \quad (8)$$

where we have used the normalization $\langle \Psi_{E,k} | \Psi_{E,k} \rangle = 1$. Together with Eq. (7) we find that particles with $E > 0$ and holes with $E < 0$ have the opposite current (and group velocity); i.e., all particles (with $k > -A_{\min}$) move to the right and all holes move to the left. In this way, one obtains a (nearly) perfect charge separation.

Asymptotics.—It is illustrative to study the limiting cases where $|k|$ is large compared to the scales set by the magnetic field (but still well below the inverse lattice spacing). For large and positive k , the potential \mathcal{V}_k can be approximated by $\mathcal{V}_k \approx k^2 + 2kA(x)$. Thus, to lowest order in k , we obtain $E \approx \pm v_F k$; i.e., these modes propagate with a speed close to the Fermi velocity. Going to the next order in k , we may expand $A(x)$ around its minimum at x_0 , where the magnetic field $B(x_0) = 0$ vanishes $A(x) \approx A_{\min} + A''(x_0)(x - x_0)^2/2$ and obtain harmonic oscillator eigenfunctions centered at x_0 [assuming that $A''(x_0) = B'(x_0) \neq 0$]. Since the stiffness of the potential behaves as $kB'(x_0)$, the modes are strongly localized around x_0 for large k and basically propagate along the x_0 line where the magnetic field vanishes. For fixed and large k , these modes have equidistant values of E where the distance scales with $\sqrt{B'(x_0)}$.

For large and negative k values, the minima of the potential \mathcal{V}_k are given by $A(x_\pm) + k = 0$ and thus the modes are localized at large and nearly opposite values of $x_\pm \sim \pm|k/B_0|$ due to $A(x \rightarrow \pm\infty) \sim B_0|x|$. In this regime, $A(x)$ is approximately linear and thus we recover the harmonic oscillator eigenfunctions corresponding to the usual (pseudorelativistic) Landau levels in a constant magnetic field [18]. Note, however, that the eigenfunctions $\psi_1^{E,k}(x)$ are linear superpositions of the Landau levels centered at x_+ and x_- with the same energy E . In this limit, the eigenenergies E do not depend on k anymore ($E_L^n = \pm v_F \sqrt{2B_0 n}$ with $n \in \mathbb{N}$) and thus the current J^y also vanishes. Hence these modes are not so interesting for our purpose.

Matrix elements.—Now we are in the position to study the excitation of particle-hole pairs by incident photons (in the infrared or optical regime). In second quantization, the interaction Hamiltonian reads

$$\hat{H}_{\text{int}} = \int dx dy \hat{\Psi}^\dagger \gamma^\mu \hat{A}_\mu \hat{\Psi}, \quad (9)$$

where the photon field operator \hat{A}_μ contains the creation and annihilation operators $\hat{a}_{\omega,k,\sigma}^\dagger$ and $\hat{a}_{\omega,k,\sigma}$ for frequency ω , wave number k , and polarization σ . The Dirac field

operator $\hat{\Psi}$ is a linear combination of the annihilation operators for particles $\hat{c}_{E>0,k}^\dagger \Psi_{E>0,k}$ and the creation operators for holes $\hat{c}_{E'<0,k'}^\dagger \Psi_{E'<0,k'}$.

If we now consider the transition matrix elements $\langle \text{out} | \hat{U}_{\text{int}} | \text{in} \rangle$ with an initial photon $|\text{in}\rangle = \hat{a}_{\omega,k,\sigma}^\dagger |0\rangle$ and a final particle-hole pair $|\text{out}\rangle = \hat{c}_{E>0,k}^\dagger \hat{c}_{E'<0,k'}^\dagger |0\rangle$, we get to first order in perturbation theory

$$\mathfrak{M}_{E,k;E',k'}^{\omega,k,\sigma} = \frac{1}{\sqrt{2\omega}} \int dt dx dy \bar{\Psi}_{E,k} \gamma^\mu A_\mu^\sigma \Psi_{E',k'} \times e^{+iEt -iky} e^{-i\omega t + ik \cdot r} e^{-iE't + ik'y}, \quad (10)$$

where A_μ^σ encodes the polarization of the photon. As usual, the t integral gives $\delta(\omega - E + E')$, i.e., energy conservation. Since the wavelength of the photons under consideration (in the optical or infrared regime) is much larger than the typical length scales of the electronic modes in graphene, we may neglect the photon wave number k . Therefore, the y integral yields $\delta(k - k')$; i.e., we excite particle-hole pairs with the same wave number $k = k'$. The remaining x integral reads

$$\mathfrak{M}_{E,k;E',k'=k}^{\omega=E-E',k \approx 0,\sigma} \propto \int dx \bar{\Psi}_{E,k} \gamma^\mu A_\mu^\sigma \Psi_{E',k}. \quad (11)$$

Let us first assume $A_\mu^\sigma = \text{const}$ and consider the transition between modes of the same E^2 (i.e., $E = -E'$), such as the uppermost negative mode (for a given k) and the lowermost positive mode (cf. Fig. 2). In this case, we may use the aforementioned particle-hole symmetry $\Psi_{-E,k} = \sigma^z \Psi_{E,k}$ and simplify the integrand via $\bar{\Psi}_{E,k} \gamma^\mu \Psi_{E',k} = \bar{\Psi}_{E,k} \gamma^\mu \sigma^z \Psi_{E,k}$. Inserting $\gamma^1 = i\sigma^y$ and $\gamma^2 = -i\sigma^x$ and using the properties of the Pauli matrices, we see that the matrix element for the photon polarization in the x direction A^x yields the same expression as in the current J^y [cf. Eq. (5)] and vice versa. Consequently, the matrix elements (11) vanish for the photon polarization in the y direction, but yield a nonzero contribution for the photon polarization in the x direction, at least if k is large enough [cf. the discussion after Eq. (7)]. Moreover, the modes with

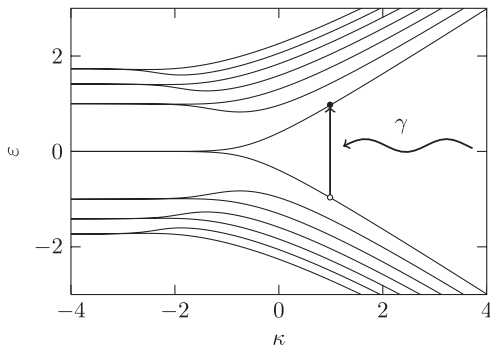


FIG. 2. Dispersion relation of the lowest bands with $\kappa = k \ell_B$ and $E = \varepsilon v_F \sqrt{2B_0}$ and sketch of the photoabsorption.

large currents J_y and thus large group velocities dE/dk also have large matrix elements, which enhances the magnetophotovoltaic or magnetothermoelectric effect we are interested in.

Pseudoparity.—Further selection rules arise if we assume reflection symmetry $B(-x) = -B(x)$ and thus $A(-x) = A(x)$ which yields the additional symmetry

$$\psi_1^{E,k}(-x) = \pm i \psi_2^{E,k}(x) = i \mathcal{P}_{E,k} \psi_2^{E,k}(x), \quad (12)$$

where we call $\mathcal{P}_{E,k} = \pm 1$ the pseudoparity of this mode. Recalling the particle-hole symmetry $\Psi_{-E,k} = \sigma^z \Psi_{E,k}$, we find $\mathcal{P}_{-E,k} = -\mathcal{P}_{E,k}$. The pseudoparity of a given mode can be determined easily for large and positive k , where we have $i \psi_2^{E,k} \approx v_F k \psi_1^{E,k} / E$ from Eq. (3). Since the wave function $\psi_1^{E,k}(x)$ of the lowest positive mode (for large and positive k) corresponds to the ground state of a harmonic oscillator, it is Gaussian and symmetric $\psi_1^{E,k}(-x) = \psi_1^{E,k}(x)$. Hence this mode has an even pseudoparity $\mathcal{P}_{E,k} = +1$. The wave function $\psi_1^{E,k}(x)$ of the next mode corresponds to the first excited state of a harmonic oscillator and thus is antisymmetric $\psi_1^{E,k}(-x) = -\psi_1^{E,k}(x)$, which gives an odd pseudoparity $\mathcal{P}_{E,k} = -1$ and so on. Together with the above result $\mathcal{P}_{-E,k} = -\mathcal{P}_{E,k}$ we find that, for a fixed k , the pseudoparity of the modes alternates if we go up and down in energy. Assuming that the modes deform continuously if k changes [i.e., that $A(x)$ is sufficiently well behaved], we may deduce an alternating pseudoparity for all k .

Now, the integrand in the matrix elements (11) behaves as $\psi_1^{E,k}(x) \psi_2^{E',k}(x) \pm \psi_2^{E,k}(x) \psi_1^{E',k}(x)$ for the two photon polarizations. Inserting Eq. (12) and integrating over x , we see that the matrix elements (11) between modes of the same pseudoparity vanish for photon polarizations in the x direction whereas the transition between modes of opposite pseudoparity is forbidden for the other polarization.

Yet another set of selection rules can be obtained in the asymptotic regimes. For large and positive k we only get transitions between modes of opposite energies (due to the orthogonality of the harmonic oscillator eigenfunctions). In the opposite limit (large and negative k), we recover the well-known [18] properties of the Landau levels $E_L^n = \pm v_F \sqrt{2B_0} n$ with $n \in \mathbb{N}$ where we only get transitions for $n \rightarrow n \pm 1$.

Polarization dependence.—So far, we have discussed the case $A_\mu^\sigma = \text{const}$ in Eq. (11). This is certainly a good approximation if the polarization of the incident photon points in the y direction, i.e., is aligned with the symmetry of our setup. However, for the other (x) polarization, A_μ^σ in Eq. (11) should be replaced by the local projection of the photon wave function A_μ^σ onto the graphene plane, i.e., become x dependent $A_\mu^\sigma(x)$. The profile of $A_\mu^\sigma(x)$ then depends on the incidence angle of the photon. If the photon is incident from the top, i.e., propagates parallel to the

external magnetic field $\mathbf{k} \parallel \mathbf{B}$, the two graphene sheets (top and bottom) have opposite projections. Thus $A_\mu^\sigma(x)$ is antisymmetric $A_\mu^\sigma(-x) = -A_\mu^\sigma(x)$ and the above selection rules are reversed. If the photon propagates perpendicularly through the fold ($\mathbf{k} \perp \mathbf{B}$), we get a symmetric projection function $A_\mu^\sigma(-x) = A_\mu^\sigma(x)$ which vanishes far away from the folding region (i.e., for large $|x|$). In this case, the above selection rules do still apply, but the matrix elements might be reduced a bit.

Example profile.—In order to visualize the behavior of the modes by means of a concrete example, let us consider a magnetic field of the following form

$$B(x) = B_0 \tanh(\alpha x), \quad (13)$$

where $1/\alpha$ measures the width of the fold. For $\alpha \rightarrow \infty$, we get a step function $B(x) = B_0 \text{sgn}(x)$ with the vector potential $A(x) = B_0|x|$ (cf. Ref. [19]). In this limit, the mode equation (3) can be solved exactly (piecewise) in terms of parabolic cylinder functions (cf. Ref. [20]). Incidentally, the spectrum for such a step function $B(x) = B_0 \text{sgn}(x)$ can also arise for some edge states [12,13].

However, such a step function can only be a good approximation if k is not too large and if the curvature radius of the graphene fold is much smaller than the typical magnetic length scale $\ell_B = 1/\sqrt{B}$. For 1 T, we get $\ell_B \approx 26$ nm while the radius of curvature cannot be too small since it should be much larger than the lattice spacing ≈ 0.25 nm. Thus, let us consider a finite α and take $\alpha = 1/\ell_B$ as an example. The spectrum can then be obtained numerically and is given in Fig. 2. The spectra for other values of α are qualitatively similar. As demonstrated above, the two lowest modes are monotonically increasing or decreasing, whereas the higher modes can have $dE/dk = 0$ at some small k values. For large $|k|$, we recover the asymptotics discussed above.

Conclusions.—Via the effective Dirac equation (1), we studied the low-energy behavior of electronic excitations in graphene under the influence of a transversal magnetic field $B(x)$ with the asymptotics $B(x \rightarrow \pm\infty) = \pm B_0$. Such a field profile $B(x)$ arises within a folded graphene sheet in a constant magnetic field (for example, see Fig. 1). Based on general arguments, we find a discrete set of modes (see also Ref. [21]) which are localized near the fold (i.e., the zero of the magnetic field) and propagate along it with a significant fraction of the Fermi velocity.

Due to particle-hole symmetry, the dispersion relations $E(k)$ of these modes (cf. Fig. 2) are symmetric around the $E = 0$ axis, but never cross it. Thus, these modes have a finite energy gap (for each k) with the characteristic energy scale being set by the (pseudorelativistic) Landau level energy $E_L = v_F \sqrt{2B_0}$. For a magnetic field of 1 T, we have $E_L \approx 36$ meV, which corresponds to 400 K. The group velocity dE/dk is related to the current J^y and we find that particles and holes move in opposite directions. Apart from some minor exceptions, all particles move to

the right and all holes move to the left—i.e., we get a nearly perfect charge separation. In view of this predetermined direction, the finite energy gap, and the fact that these localized modes are qualitatively independent of the shape of $A(x)$, we expect that they are quite robust against perturbations. In addition, we consider the propagation within a (curved) graphene sheet, i.e., far away from any edges with defects, etc.

Finally, we study the excitation of particle-hole pairs in these modes via incident infrared or optical photons, i.e., magnetophotovoltaic or magnetothermoelectric effects. The matrix elements (10) display a distinct dependence on the polarization and the incidence angle of the photons, which should enable us to distinguish this effect from other phenomena experimentally. Furthermore, we find that those modes with comparably large group velocities (i.e., large currents) tend to have large matrix elements (at least for low-energy transitions) and thus are more strongly coupled to the incident photons—i.e., “nature favors our goal.”

Outlook: electric field.—If we apply an additional electric field perpendicular to the fold and the magnetic field, we get an electrostatic potential $\Phi(x) = \beta v_F A(x)$ with some constant β . If we have $|\beta| < 1$ (i.e., if the electric field is subcritical), we may transform Φ away by an effective Lorentz boost in the y direction with a velocity $v_{\text{boost}} = \beta v_F$ where v_F plays the role of the speed of light [22]. In the Lorentz boosted frame, we get the same modes as discussed above, but with a reduced magnetic field $B'_0 = B_0 \sqrt{1 - \beta^2}$. Since this field enters the characteristic energy scale via $v_F \sqrt{2B_0}$, the dispersion relation after transforming back to laboratory coordinates reads

$$E \rightarrow E' = E(1 - \beta^2)^{3/4} - k v_F \beta; \quad (14)$$

i.e., the spectrum in Fig. 2 is compressed and tilted.

Fruitful discussions with A. Lorke and M. Schleberger are gratefully acknowledged. This work was supported by DFG (SFB-TR12).

*ralf.schuetzhold@uni-due.de

- [1] A. von Ettingshausen and W. Nernst, *Ann. Phys. (N.Y.)* **265**, 343 (1886).
- [2] M. O. Goerbig, *Rev. Mod. Phys.* **83**, 1193 (2011); A. H. C. Neto, F. Guinea, N. M. R. Peres, K. S. Novoselov, and A. K. Geim, *Rev. Mod. Phys.* **81**, 109 (2009); S. Das Sarma, S. Adam, E. H. Hwang, and E. Rossi, *Rev. Mod. Phys.* **83**, 407 (2011).
- [3] M. I. Katsnelson, I. V. Grigorieva, S. V. Dubonos, and A. A. Firsov, *Nature (London)* **438**, 197 (2005).
- [4] K. S. Novoselov, A. K. Geim, S. V. Morozov, D. Jiang, Y. Zhang, S. V. Dubonos, I. V. Grigorieva, and A. A. Firsov, *Science* **306**, 666 (2004).
- [5] Y. Zhang, Y.-W. Tan, H. L. Stormer, and P. Kim, *Nature (London)* **438**, 201 (2005); D. A. Abanin, K. S. Novoselov,

- U. Zeitler, P. A. Lee, A. K. Geim, and L. S. Levitov, *Phys. Rev. Lett.* **98**, 196806 (2007).
- [6] P. R. Wallace, *Phys. Rev.* **71**, 622 (1947).
- [7] J. G. Checkelsky and N. P. Ong, *Phys. Rev. B* **80**, 081413 (R) (2009); Z. Zhu, H. Yang, Benoît Fauqué, Y. Kopelevich, and K. Behnia, *Nat. Phys.* **6**, 26 (2009); Y. M. Zuev, W. Chang, and P. Kim, *Phys. Rev. Lett.* **102**, 096807 (2009); P. Wei, W. Bao, Y. Pu, C. N. Lau, and J. Shi, *Phys. Rev. Lett.* **102**, 166808 (2009).
- [8] L. Zhu, R. Ma, L. Sheng, M. Liu, and D. N. Sheng, *Phys. Rev. Lett.* **104**, 076804 (2010); I. A. Luk'yanchuk, A. A. Varlamov, and A. V. Kavokin, *Phys. Rev. Lett.* **107**, 016601 (2011); E. H. Hwang, E. Rossi, and S. Das Sarma, *Phys. Rev. B* **80**, 235415 (2009).
- [9] E. Prada, P. San-Jose, and L. Brey, *Phys. Rev. Lett.* **105**, 106802 (2010); D. Rainis, F. Taddei, M. Polini, G. León, F. Guinea, and V. I. Fal'ko, *Phys. Rev. B* **83**, 165403 (2011); N. Yang, X. Ni, J.-W. Jiang, and B. Li, *Appl. Phys. Lett.* **100**, 093107 (2012).
- [10] S. Akcöltekin, H. Bukowska, T. Peters, O. Osmani, I. Monnet, I. Alzahr, B. Ban d'Etat, H. Lebius, and M. Schleberger, *Appl. Phys. Lett.* **98**, 103103 (2011); J. Zhang, J. Xiao, X. Meng, C. Monroe, Y. Huang, and J.-M. Zuo, *Phys. Rev. Lett.* **104**, 166805 (2010); S. Cranford, D. Sen, and M. J. Buehler, *Appl. Phys. Lett.* **95**, 123121 (2009); J.-H. Yoo, J. B. In, J. B. Park, H. Jeon, and C. P. Grigoropoulos, *Appl. Phys. Lett.* **100**, 233124 (2012); L. Ortolani, E. Cadelano, G. P. Veronese, C. D. E. Boschi, E. Snoeck, L. Colombo, and V. Morandi, *Nano Lett.* **12**, 5207 (2012); K. Kim, Z. Lee, B. D. Malone, K. T. Chan, B. Aleman, W. Regan, W. Gannett, M. F. Crommie, M. L. Cohen, and A. Zettl, *Phys. Rev. B* **83**, 245433 (2011).
- [11] M. Fujita, K. Wakabayashi, K. Nakada, and K. Kusakabe, *J. Phys. Soc. Jpn.* **65**, 1920 (1996); K. Nakada, M. Fujita, G. Dresselhaus, and M. S. Dresselhaus, *Phys. Rev. B* **54**, 17954 (1996); K. Kim, V. I. Artyukhov, W. Regan, Y. Liu, M. F. Crommie, B. I. Yakobson, and A. Zettl, *Nano Lett.* **12**, 293 (2012).
- [12] S. Park and H.-S. Sim, *Phys. Rev. B* **77**, 075433 (2008); D. A. Abanin, P. A. Lee, and L. S. Levitov, *Phys. Rev. Lett.* **96**, 176803 (2006); N. M. R. Peres, A. H. Castro Neto, and F. Guinea, *Phys. Rev. B* **73**, 241403(R) (2006); K. Wakabayashi, M. Fujita, H. Ajiki, and M. Sigrist, *Phys. Rev. B* **59**, 8271 (1999); S. Wu, M. Killi, and A. Paramekanti, *Phys. Rev. B* **85**, 195404 (2012); J. A. M. van Ostaay, A. R. Akhmerov, C. W. J. Beenakker, and M. Wimmer, *Phys. Rev. B* **84**, 195434 (2011); N. M. R. Peres, F. Guinea, and A. H. Castro Neto, *Phys. Rev. B* **73**, 125411 (2006); H. A. Fertig and L. Brey, *Phys. Rev. Lett.* **97**, 116805 (2006); D. A. Abanin, P. A. Lee, and L. S. Levitov, *Solid State Commun.* **143**, 77 (2007); P. Delplace and G. Montambaux, *Phys. Rev. B* **82**, 205412 (2010); I. Romanovsky, C. Yannouleas, and U. Landman, *Phys. Rev. B* **83**, 045421 (2011).
- [13] R. Ribeiro, J.-M. Poumirol, A. Cresti, W. Escoffier, M. Goiran, J.-M. Broto, S. Roche, and B. Raquet, *Phys. Rev. Lett.* **107**, 086601 (2011); S. Minke, S. H. Jhang, J. Wurm, Y. Skourski, J. Wosnitza, C. Strunk, D. Weiss, K. Richter, and J. Eroms, *Phys. Rev. B* **85**, 195432 (2012).
- [14] G. W. Semenoff, *Phys. Rev. Lett.* **53**, 2449 (1984).
- [15] Note that Eq. (1) describes the vicinity of one Dirac point (say K), but the behavior of the other Dirac point (K') is completely analogous (up to an internal rotation). In addition, the real spin degree of freedom of the electrons is neglected (as usual) since the associated energy scale is too small, i.e., both spin species (spin up and down) again behave approximately in the same way.
- [16] Of course, the presence of the two metallic leads at the ends of the fold eventually breaks the translation symmetry. However, if the two leads are sufficiently far apart and their conductance and connection to the folded graphene sheet is good enough, the continuum description used here should be a good approximation.
- [17] R. Courant and D. Hilbert, *Methoden der Mathematischen Physik* (Springer, Berlin, 1924).
- [18] V. P. Gusynin and S. G. Sharapov, *Phys. Rev. Lett.* **95**, 146801 (2005); M. L. Sadowski, G. Martinez, M. Potemski, C. Berger, and W. A. de Heer, *Phys. Rev. Lett.* **97**, 266405 (2006).
- [19] L. Dell'Anna and A. De Martino, *Phys. Rev. B* **79**, 045420 (2009); A. De Martino, L. Dell'Anna, and R. Egger, *Phys. Rev. Lett.* **98**, 066802 (2007).
- [20] S. Kuru, J. Negro, and L. M. Nieto, *J. Phys. Condens. Matter* **21**, 455305 (2009).
- [21] T. K. Ghosh, A. De Martino, W. Häusler, L. Dell'Anna, and R. Egger, *Phys. Rev. B* **77**, 081404(R) (2008); L. Oroszlány, P. Rakyta, A. Kormányos, C. J. Lambert, and J. Cserti, *Phys. Rev. B* **77**, 081403(R) (2008); J. R. Williams and C. M. Marcus, *Phys. Rev. Lett.* **107**, 046602 (2011).
- [22] V. Lukose, R. Shankar, and G. Baskaran, *Phys. Rev. Lett.* **98**, 116802 (2007).